Lyapunov-based Controller using Singular Perturbation Theory : An Application on a mini-UAV

Gerardo Ramon Flores Colunga, Rogelio Lozano

2013 American Control Conference (ACC)
Washington, DC, USA, June 17-19, 2013

Lyapunov-based Controller using Singular Perturbation Theory: An Application on a mini-UAV

Gerardo Flores† and R. Lozano⋆

Abstract— **In this paper, a Lyapunov-based control using singular perturbation theory is proposed and applied on dynamics of a miniature unmanned aerial vehicle (MAV). Such controller is designed taking into account the presence of the small parameter ϵ on vehicle dynamics, causing a time-scale separation between the attitude and translational dynamics of the MAV. The stability analysis is demonstrated by presenting a scenario in which the time-scale property arises on the the MAV dynamics. In addition, the values of the parameter ϵ for which the control law is validated, are given. Simulations are derived an presented to demonstrate the effectiveness of the control law. The proposed controller has been applied to a *Quad-plane* MAV experimental platform, in order to validate the performance and to show the time-scale property.**

I. Introduction

The growing development of technologies like microcomputers, vision systems, IMU's and other sensor devices, has increased the interest and research on MAVs. As a consequence, the control and robotics community have been interested on developing controllers that can deal with the complexity of the MAV dynamics.

It is well known that the sub-actuated dynamics of the MAV has a fast dynamics formed by the orientation subsystem, and a slow dynamics formed by the translational subsystem [1], [2]. Thus, the stabilization and tracking trajectory problem on a MAV can be addressed by using of the fact that, there exists a time scale separation between the translational and rotational dynamics, leading to a hierarchical control. The hierarchical control scheme presents two or more separate controllers that can be designed separately to successively stabilize the dynamics of the vehicle, and can be used in order to design position and orientation controllers leading to simplify the problem.

In recent papers [3], [4], [5] the use of a hierarchical control structure has been treated, exploiting the fact that there exists a time scale separation between MAV translational and rotational dynamics, latter being the fast dynamics of the system. However, the vast majority of the works only make mention of this feature, and do not address the problem in a theoretical point of view, using tools like the singular perturbation theory.

Some researchers have exploited the aforementioned hierarchical structure [1], [3], [4], [5], [6], [7], but they use the time scale separation just to justify the implementation of two different controllers: a controller for the attitude subsystem and a controller for the translational subsystem. However, they do not use a singular perturbation structure on MAV dynamics, to show the time-scale property. This is because in general, the presence of such property makes the problem hard from the numerical solution point of view [8]. However, in a few works [9], [10] such phenomena is pointed out justifying the time-scale separation property.

In this paper, we present a stabilization analysis of the MAV dynamics in the six degrees of freedom, by using the singular perturbation theory. The considered system presents a not pure strict-feedback structure, and the control vectors formed by the force and trust have a different relative degree w.r.t. MAV position. In order to overcome this difficulty we propose to use a dynamic extension on the force control vector. Furthermore, an analysis of the system is considered by introducing the parameter ϵ on the MAV dynamics, in order to illustrate the time-scale separation between the attitude and translational dynamics of the MAV. The proposed control law should be tested at simulation level, and be implemented on an experimental platform.

The paper is organized as follows. In Section II the problem description and the singular perturbed problem are introduced. The MAV model is presented as a singular perturbation structure in Section III. In section IV the controller is developed and the corresponding stability proof is derived. Simulations are given in Section V, in order to prove the proper operation of the control law. In addition, experimental results tested on the *Quad-plane* MAV platform [4], are shown. Finally, some conclusions are drawn in Section VI.

II. Problem Description

Singular perturbation and hence, the time-scale character is often associated with a small parameter ϵ, multiplying some of the state variables of the considered system. One difficult is that such parameter does not appear in the desired form or it may not be identifiable at all. Frequently, only by past experience and physical insights, one can know that a particular system has fast and slow modes. In the cases where it is impossible to identify the parameter ϵ, one can artificially introduce ϵ to be associate with the fast dynamics.

There exist three different approaches for the selection of time scales [8]: linearization of the state equations, transformation of the state equations and direct identification of small parameters. However, in many aerospace problems, no singular parameter appears explicitly on the dynamic equations. In such cases, the parameter ϵ may be artificially inserted for presenting a singular perturbation structure,

This work was partially supported by the Institute for Science & Technology of Mexico City (ICyTDF).

† is with the Heudiasyc UMR 6599 Laboratory, University of Technology of Compiègne, France. email: gfloresc@hds.utc.fr

⋆ is with the Heudiasyc UMR 6599 Laboratory, UTC CNRS France and LAFMIA UMI 3175, Cinvestav, México. email: rlozano@hds.utc.fr

which is shown below

$$\begin{aligned} \dot{x} &= f(x,z,u) \\ \epsilon\dot{z} &= g(x,z,u) \end{aligned} \tag{1}$$

where $x \in \Re^n$, $z \in \Re^m$, f and g are smooth functions, $u \in \Re^r$ is a control input and $\epsilon \in (0,1]$.

The first goal of the paper is to present the MAV mathematical model as a singular perturbation structure, as in (1). Then, we proceed to design a Lyapunov-based control law, which stabilizes the vehicle on a predefined three-dimensional position. The second goal is to investigate the ϵ values in which the proposed control can be implemented.

III. System Description

In this section, an idealized mathematical model of the MAV is described. Such model will be suitable for developing the purposed control law. We will consider the nonlinear rigid body dynamics in terms of rotational and translational dynamics [11] given by

$$\begin{aligned} \dot{\xi} &= \upsilon \\ \dot{\upsilon} &= \tfrac{RF}{m} - ge_{z_\mathcal{I}} \\ \dot{R} &= R\mathrm{S}(\Omega) \\ \dot{\Omega} &= -J^{-1}\Omega \times J\Omega + J^{-1}\tau \end{aligned} \tag{2}$$

where $\xi = (x,y,z)^T$ and $\upsilon = (v_x, v_y, v_z)^T$ are respectively, position and velocity of the MAV relative to the inertial frame $\mathcal{I} = (e_{x_\mathcal{I}}, e_{y_\mathcal{I}}, e_{z_\mathcal{I}})$. $R \in SO(3)$ is the rotational matrix representing MAV orientation in body coordinate frame $\mathcal{B} = (e_{x_\mathcal{B}}, e_{y_\mathcal{B}}, e_{z_\mathcal{B}})$ w.r.t. $\mathcal{I}$, $\Omega \in \Re^3$ is the body angular velocity vector. $F \in \Re^3$ and $\tau \in \Re^3$ are the force and torque, respectively applied at the center of mass of the MAV and specified w.r.t. $\mathcal{B}$. $J \in \Re^3$ is the inertia matrix, m is the mass of the body, $ge_{z_\mathcal{I}}$ is the gravitational force and $e_{z_\mathcal{I}} = (0,0,1)$ is a unit vector. In (2), $SO(3)$ denotes the special orthogonal group of $\Re^{3\times 3}$, and $so(3)$ is the group of antisymmetric matrices of $\Re^{3\times 3}$. Also, we define by $S(v)$ the operator from $\Re^3 \to so(3)$ such that

$$\forall v \in \Re^3, S(v) = \begin{pmatrix} 0 & -v_3 & v_2 \\ v_3 & 0 & -v_1 \\ -v_2 & v_1 & 0 \end{pmatrix} \tag{3}$$

where v_i denotes the ith component of vector v. Thus, $S(v)\Omega = v \times \Omega$.

It is important to note that the dynamic model (2) is not in pure strict-feedback structure, and control vectors F and τ have different relative degree w.r.t. the position ξ. For this reason we take the dynamic extension of control F as

$$\ddot{F} = \tilde{F} \tag{4}$$

In this way, the actual control F and its first time derivative $\dot{F}$, become internal variables of a dynamic controller [12]. Thus, it is possible to represent (2) as

$$\begin{aligned} \dot{\xi} &= \upsilon \\ \dot{\upsilon} &= X \\ \dot{X} &= Y \\ \dot{Y} &= \tfrac{R}{m}\left(\tilde{F} - S(F)\tilde{\tau} + 2S(\Omega)\dot{F} + S(\Omega)S(\Omega)F\right) \end{aligned} \tag{5}$$

where new states X, Y and control input $\tilde{\tau}$ are defined as

$$\begin{aligned} X &:= \tfrac{RF}{m} - ge_{z_\mathcal{I}} \\ Y &:= \dot{X} = \tfrac{R}{m}(S(\Omega)F + \dot{F}) \\ \tilde{\tau} &:= \dot{\Omega} \end{aligned} \tag{6}$$

Thereby, new inputs $\tilde{F}, \tilde{\tau}$ have a relative degree equal to four w.r.t. the state ξ. Thus, they can be assigned at the same stage, eliminating the problem of the presence of an aggressive control, which may lead to extreme ill-conditioning of the remaining closed-loop system [13].

A. Modeling for the Singular Perturbation Problem

In many MAV problems or more generally, in more aerospace problems, no singular perturbation parameter appears explicitly on the mathematical model. In such cases, a singular perturbation parameter may be artificially inserted to define a rapid response of a certain dynamic w.r.t. other. In other cases, this parameter is may be inserted to suppress the variables in the equations that are expected to have relatively negligible effects.

The slow-fast time scale character is often associate with a small parameter multiplying some of the state variables of the state equations describing a physical system. However, often that parameter may not be identifiable at all and only by physical insight and past experiences does one know that the system has fast and slow dynamics.

Experience indicates that among the state variables, the position and velocity are slow relative to the dynamic of the Euler angles. It is this separation of the states velocities, that motivates to formulate a singular perturbation structure as follows

$$\begin{aligned} \dot{\xi} &= \upsilon \\ \dot{\upsilon} &= X \\ \epsilon\dot{X} &= Y \\ \epsilon\dot{Y} &= \tfrac{R}{m}\left(\tilde{F} - S(F)\tilde{\tau} + 2S(\Omega)\dot{F} + S(\Omega)S(\Omega)F\right) \end{aligned} \tag{7}$$

IV. Controller Design

In this section we will propose a control strategy for stabilization of (7). The controller will be successively designed as presented below.

From the last equation of (7) we can write

$$\frac{R}{m}\left(\tilde{F} - S(F)\tilde{\tau} + 2S(\Omega)\dot{F} + S(\Omega)S(\Omega)F\right) = u \tag{8}$$

where u will be taken as control input. By adding $X + Y$ in both sides of (8), this equation stays in balance, then we get a feedback connection in (7) as follows

$$\dot{\xi} = \upsilon \tag{9}$$

$$\dot{\upsilon} = X \tag{10}$$

$$\epsilon\dot{X} = Y \tag{11}$$

$$\epsilon\dot{Y} = Y + X + u \tag{12}$$

To be consistent with the notation used in (1), vectors x and z are given by $x = [\xi \quad \upsilon]^T$, $z = [X \quad Y]^T$ and $f(x,z,u) = [\upsilon \quad X]^T$, $g(x,z,u) = [Y \quad Y + X + u]^T$.

The goal is to design a feedback control law which stabilizes the system (9)-(12) at the equilibrium point $\xi = 0$, $\upsilon = 0$, $X = 0$, $Y = 0$ and prove the asymptotic stability of the closed-loop system. For achieve this goal, we need to investigate a candidate Lyapunov function for such system. The key idea is to analyze the system separately, beginning with the slow subsystem (9)-(10) and continuing with the fast subsystem (11)-(12). Then, find a control for each subsystem and investigate their corresponding candidate Lyapunov functions. Finally, combining both candidate Lyapunov functions in a proper way, we find the candidate Lyapunov function for the entire system (9)-(12).

We begin by analyzing the slow system (9)-(10). Let us assume that the open-loop system (9)-(10) is a standard singularly perturbed system for every $u \in B_u \subset \Re^3$, that is to say, the equations

$$\begin{array}{rcl} 0 & = & Y \\ 0 & = & Y + X + u \end{array} \tag{13}$$

have a unique root $z = h(x, u)$.

Such control u will be composed of the sum of slow and fast controls

$$u = u_s + u_f \tag{14}$$

where

$$u_s = \Xi_s(\xi, \upsilon) \tag{15}$$

is a feedback function of the states that compose the fast system dynamics (11)-(12), and

$$u_f = \Xi_f(\xi, \upsilon, X, Y) \tag{16}$$

is a feedback function depending on the states (ξ, υ, X, Y). In order to find the control (15), we see from (13) that

$$X = -u_s \tag{17}$$

and then, we propose the slow controller u_s given by

$$u_s = k_{Ps}\xi + k_{Ds}\upsilon \tag{18}$$

Thus, with the control (18) the closed-loop reduced system (9)-(10) results in

$$\begin{array}{rcl} \dot{\xi} & = & \upsilon \\ \dot{\upsilon} & = & -k_{Ps}\xi - k_{Ds}\upsilon \end{array} \tag{19}$$

Using the candidate Lyapunov function

$$V(\xi, \upsilon) = \frac{\lambda}{2}\xi^T\xi + \frac{q}{2\lambda}\upsilon^T\upsilon + \xi^T\upsilon \tag{20}$$

with parameters $\lambda > 0$, $q > 0$ properly chosen, the derivative of (20) w.r.t. (19) is given by

$$\dot{V}(\xi, \upsilon) = -k_{Ps}\xi^T\xi - \left(\frac{q}{\lambda}k_{Ds} - 1\right)\upsilon^T\upsilon \tag{21}$$

We need to investigate a scalar function $\psi(\cdot)$ of vector arguments which vanish only when its arguments are zero, such that

$$\dot{V}(\xi, \upsilon) \leq -\alpha_1\psi^2(\xi, \upsilon) \tag{22}$$

where $\alpha_1 > 0$. The inequality (22) holds with the scalar function

$$\psi(\xi, \upsilon) = \left\| \begin{pmatrix} |\xi| \\ \rho|\upsilon| \end{pmatrix} \right\| \tag{23}$$

where$\|\cdot\|$ is the Euclidean norm of a vector and ρ is an arbitrary positive number to be chosen.

The boundary layer model [14] of the closed-loop system (9)-(12) is defined as

$$\begin{array}{rcl} \frac{dX}{d\tau} & = & Y \\ \frac{dY}{d\tau} & = & X + Y + k_{Ps}\xi + k_{Ds}\upsilon + u_f \end{array} \tag{24}$$

We proceed to design a fast control law (16). One inspection of (24) suggests to chose the fast control as

$$u_f = -3(X + Y + k_{Ps}\xi + k_{Ds}\upsilon) \tag{25}$$

The control (25) needs to fulfill certain requirements for system (9)-(12) remains a standard singularly perturbed system. The first one is that $u_f = \Xi_f(\xi, \upsilon, X, Y)$ be inactive for $z = h(x, u_s)$, i.e. $\Xi_f(x, h(x, \Xi_f(x))) = 0$, then

$$\Xi_f(x, h(x, \Xi_f(x))) = -3(X+Y+k_{Ps}\xi+k_{Ds}\upsilon) = 0 \tag{26}$$

holds with $X = -k_{Ps}\xi - k_{Ds}\upsilon$ and $Y = 0$. The requirement (26) guarantees that $z = h(x, \Xi_s(x))$ is a root of

$$\begin{array}{rcl} 0 & = & Y \\ 0 & = & Y + X + u_s + u_f \end{array} \tag{27}$$

In addition, (27) should have a unique root $z = h(x, \Xi_s(x))$ in a certain domain of interest $B_x \times B_z$, which is easy to verify from (18), (25).

We proceed to investigate a candidate Lyapunov function W such that

$$\frac{\partial W}{\partial z}g(x, z, \Xi_s(x) + \Xi_f(x, z)) \leq -\alpha_2\phi^2(z - h(x, \Xi_s(x))) \tag{28}$$

$\forall (x, z) \in B_x \times B_z$, where $\alpha_2 > 0$ and $\phi(\cdot)$ is a scalar function of vector arguments which vanish only when its arguments are zero. Using the candidate Lyapunov function

$$\begin{array}{rl} W = & \frac{\lambda_w}{2}Y^TY + \frac{q_w}{2\lambda_w}(X + k_{Ps}\xi + k_{Ds}\upsilon)^T \\ & \times (X + k_{Ps}\xi + k_{Ds}\upsilon) \\ & + (Y)^T(X + k_{Ps}\xi + k_{Ds}\upsilon) \end{array} \tag{29}$$

the time derivative of (29) can be calculated as

$$\begin{array}{rl} \dot{W} = & (-2\lambda_w + 1)Y^TY \\ & + (-2\lambda_w + \frac{q_w}{\lambda_w} - 2)(Y^T)(X + k_{Ps}\xi + k_{Ds}\upsilon) \\ & - 2(X + k_{Ps}\xi + k_{Ds}\upsilon)^T(X + k_{Ps}\xi + k_{Ds}\upsilon) \end{array} \tag{30}$$

where $\lambda_w > \frac{1}{2}$ and $-2\lambda_w + \frac{q_w}{\lambda_w} - 2 < 0$. The inequality

$$\dot{W} \leq -\alpha_2\phi^2(z - h(x)) \tag{31}$$

holds with $\alpha_2 > 0$ and with the function

$$\phi(\xi, \upsilon, X, Y) = \left\| \begin{pmatrix} |X + k_{Ps}\xi + k_{Ds}\upsilon| \\ \rho_w|Y| \end{pmatrix} \right\| \tag{32}$$

where ρ_w is an arbitrary positive number, and α_2 can take the value $\alpha_2 = 1$.

In order to complete a Lyapunov function for the entire system (9)-(12), the aforementioned Lyapunov function candidates, (20) for the slow system and (29) for the fast system, should verify the next interconnection conditions

$$\begin{aligned}&\frac{\partial W}{\partial x} f(x,z,\Xi_s(x)+\Xi_f(x,z))\\&\leq \gamma\phi^2(z-h(x,\Xi_s(x)))+\beta_2\psi(x)\phi(z-h(x,\Xi_s(x)))\end{aligned} \tag{33}$$

$$\begin{aligned}&\frac{\partial V}{\partial x}[f(x,z,\Xi_s(x)+\Xi_f(x,z))-f(x,h(x,\Xi_s(x)),\Xi_s(x))]\\&\leq \beta_1\psi(x)\phi(z-h(x,\Xi_s(x)))\end{aligned} \tag{34}$$

We proceed to verify inequalities (33) and (34). Developing inequality (33) by using (23), (32) it leads to

$$\begin{aligned}&[k_{Ps}\upsilon+k_{Ds}X]^T\left[\frac{q_w}{\lambda_w}(X+k_{Ps}\xi+k_{Ds}\upsilon)+Y\right]\\&\leq\gamma\left|X+k_{Ps}\xi+k_{Ds}\upsilon\right|^2+\gamma\rho_w^2\left|Y\right|^2\\&+\beta_2\left(\sqrt{|\xi|^2+\rho^2|\upsilon|^2}\right)\left(\sqrt{|X+k_{Ps}\xi+k_{Ds}\upsilon|^2+\rho_w^2|Y|^2}\right)\end{aligned} \tag{35}$$

adding and subtracting the term $k_{Ds}[k_{Ps}\xi+k_{Ds}\upsilon]^T\left[\frac{q_w}{\lambda_w}(X+k_{Ps}\xi+k_{Ds}\upsilon)+Y\right]$ to the LHS of (35) and by using the triangle inequality, it leads to

$$\begin{aligned}&\frac{\partial W}{\partial x} f(x,z,\Xi_s(x)+\Xi_f(x,z))\leq\\&|k_{Ps}\upsilon+k_{Ds}(-k_{Ps}\xi-k_{Ds}\upsilon)|\left|\frac{q_w}{\lambda_w}(X+k_{Ps}\xi+k_{Ds}\upsilon)+Y\right|\\&+k_{Ds}\left|X+k_{Ps}\xi+k_{Ds}\upsilon\right|\left|\frac{q_w}{\lambda_w}(X+k_{Ps}\xi+k_{Ds}\upsilon)+Y\right|\end{aligned} \tag{36}$$

Thus, if we can verify that

$$\begin{aligned}&k_{Ds}\left|X+k_{Ps}\xi+k_{Ds}\upsilon\right|\left|\frac{q_w}{\lambda_w}(X+k_{Ps}\xi+k_{Ds}\upsilon)+Y\right|\leq\\&\gamma\left|X+k_{Ps}\xi+k_{Ds}\upsilon\right|^2+\gamma\rho_w^2\left|Y\right|^2\end{aligned} \tag{37}$$

and

$$\begin{aligned}&|k_{Ps}\upsilon+k_{Ds}(-k_{Ps}\xi-k_{Ds}\upsilon)|\left|\frac{q_w}{\lambda_w}(X+k_{Ps}\xi+k_{Ds}\upsilon)+Y\right|\\&\leq\beta_2\left(\sqrt{|\xi|^2+\rho^2|\upsilon|^2}\right)\left(\sqrt{|X+k_{Ps}\xi+k_{Ds}\upsilon|^2+\rho_w^2|Y|^2}\right)\end{aligned} \tag{38}$$

hold, then the inequality (33) holds.

We proceed to prove (37). A simple calculation leads to $\frac{\gamma}{k_{Ds}}\geq 1.21$ and $\frac{q_w}{\lambda_w}\leq\rho_w^2$ which verify (37). For the inequality (38) is satisfied, we need to verify that

$$|k_{Ps}\upsilon+k_{Ds}(-k_{Ps}\xi-k_{Ds}\upsilon)|\leq\beta_{21}\left(\sqrt{|\xi|^2+\rho^2|\upsilon|^2}\right) \tag{39}$$

and

$$\begin{aligned}&\left|\frac{q_w}{\lambda_w}(X+k_{Ps}\xi+k_{Ds}\upsilon)+Y\right|\\&\leq\beta_{22}\left(\sqrt{|X+k_{Ps}\xi+k_{Ds}\upsilon|^2+\rho_w^2|Y|^2}\right)\end{aligned} \tag{40}$$

hold, where $\beta_2=\beta_{21}\beta_{22}$. Inequality (39) verifies with $\beta_{21}\geq(k_{Ps}k_{Ds})(k_{Ps}+k_{Ds}^2)$, and (40) verifies with $\beta_{22}\geq\frac{q_w}{\lambda_w}$.

We proceed to develop (34) as

$$\begin{aligned}&\left|\frac{q}{\lambda}\upsilon+\xi\right|\left|X+k_{Ps}\xi+k_{Ds}\upsilon\right|\leq\\&\beta_1\left(\sqrt{|\xi|^2+\rho^2|\upsilon|^2}\right)\left(\sqrt{|X+k_{Ps}\xi+k_{Ds}\upsilon|^2+\rho_w^2|Y|^2}\right)\end{aligned} \tag{41}$$

which can be broken up into

$$\left|\frac{q}{\lambda}\upsilon+\xi\right|\leq\beta_{11}\left(\sqrt{|\xi|^2+\rho^2|\upsilon|^2}\right) \tag{42}$$

and

$$\begin{aligned}&|X+k_{Ps}\xi+k_{Ds}\upsilon|\leq\\&\beta_{12}\left(\sqrt{|X+k_{Ps}\xi+k_{Ds}\upsilon|^2+\rho_w^2|Y|^2}\right)\end{aligned} \tag{43}$$

where $\beta_1=\beta_{11}\beta_{12}$. Inequality (42) is satisfied with $\frac{q}{\lambda}\leq\rho^2$ and $\beta_{11}\geq 2$. Inequality (43) verifies with $\beta_{12}\geq 1$.

In order to prove stability of the system (9)-(12) together with controller (14) composed by (18) and (25), we choose a candidate Lyapunov function given by

$$\nu(\xi,\upsilon,X,Y)=(1-d)V(\xi,\upsilon)+dW(X,Y) \tag{44}$$

where $d\in(0,1)$. The derivative of (44) along the closed-loop system (9)-(12)-(14) is given by

$$\dot{\nu}\leq(1-d)\frac{\partial V}{\partial x}f(x,z)+\frac{d}{\epsilon}\frac{\partial W}{\partial z}g(x,z)+d\frac{\partial W}{\partial x}f(x,z) \tag{45}$$

such Lyapunov function (45) can be represented as

$$\begin{aligned}\dot{\nu}\leq&(1-d)\frac{\partial V}{\partial x}f(x,h(x))+\\&+(1-d)\frac{\partial V}{\partial x}[f(x,z)-f(x,h(x))]\\&+\frac{d}{\epsilon}\frac{\partial W}{\partial z}g(x,z)+d\frac{\partial W}{\partial x}f(x,z)\end{aligned} \tag{46}$$

with inequalities (21), (28) and (33), (34) we get

$$\begin{aligned}\dot{\nu}\leq&-(1-d)\alpha_1\psi^2(x)+(1-d)\beta_1\psi(x)\phi(z-h(x))\\&-\frac{d}{\epsilon}\alpha_2\phi^2(z-h(x))+d\gamma\phi^2(z-h(x))\\&+d\beta_2\psi(x)\phi(z-h(x))\leq-\Phi^TA\Phi\end{aligned} \tag{47}$$

where $\Phi=[\psi(x)\quad\phi(z-h(x))]^T$ and A is given by

$$A=\begin{pmatrix}(1-d)\alpha_1 & \frac{1}{2}(1-d)\beta_1-\frac{1}{2}d\beta_2\\ \frac{1}{2}(1-d)\beta_1-\frac{1}{2}d\beta_2 & d\left(\frac{\alpha_2}{\epsilon}-\gamma\right)\end{pmatrix} \tag{48}$$

The quadratic form given in (47) is negative-definite when

$$\epsilon<\frac{\alpha_1\alpha_2}{\alpha_1\gamma+\frac{((1-d)\beta_1+d\beta_2)^2}{4d(1-d)}}:=\epsilon_d \tag{49}$$

Thus, the system (9)-(12) with the controller (14) is asymptotically stable $\forall\epsilon<\epsilon_d$.

A. Real Input Controls

In order to express the control inputs $\tilde{\tau}$ and $\tilde{F}$, let us consider the notation

$$\epsilon\dot{Y}=Z \tag{50}$$

From (7) and (12) it follows that

$$\begin{aligned}\tilde{F}-S(F)\tilde{\tau}=&mR^T(u+X+Y)-S(\Omega)F\\&-mR^TY(S(\Omega)+1)-mR^TX:=\tilde{u}\end{aligned} \tag{51}$$

where the auxiliary variable Z and the vector $\tilde{u}\in\Re^3$ are functions of known signals. Thus, using (4), (6) and (51), the original inputs F and τ can be recovered by simple calculations.

V. Numerical Simulations and Experimental Results

In this section we describe the numerical simulations and the experiments that demonstrate the effectiveness of the controller presented in section IV.

The entire fast system is comprised by the rotational dynamics composed by the states: $(\theta, \dot{\theta}, \phi, \dot{\phi}, \psi, \dot{\psi})$. The slow system is composed by the translational dynamics which is comprised by the states: $(x, \dot{x}, y, \dot{y}, z, \dot{z})$. For simplicity, we present simulations and experimental results only for two states representing the entire fast system: the roll dynamics, i.e. $(\dot{\phi}, \phi)$ and for two states representing the slow system: the lateral position dynamics, i.e. $(\dot{y}, y)$.

A. Numerical Results

In order to emphasize the time-scale separation property, and to show the faster convergence on the fast dynamics, we chose the same initial conditions for all states as $\phi(0) = \dot{\phi}(0) = y(0) = \dot{y}(0) = 3$. We have simulated the proposed controller for three different values of ϵ: $\epsilon = 0.5$, $\epsilon = 0.25$ and $\epsilon = 0.1$. In Fig. 2, the first row shows results for $\epsilon = 0.5$, the second row for $\epsilon = 0.25$ and the third row for $\epsilon = 0.1$. The simulation have been performed with the same control parameters.

The case when $\epsilon = 0.5$ is depicted in Fig. 1, and its corresponding controller in Fig. 3. The region of rapid response named boundary layer, exists near the initial point and is shown in Fig. 1. The state ϕ converges faster than the state y, and its convergence depends on the the ϵ value. From the simulations shown in Fig. 2, the rotational dynamics converge faster than the translational dynamics, according to the parameter ϵ. In addition, the boundary layer or region of rapid transition occurs near to $t = 0$.

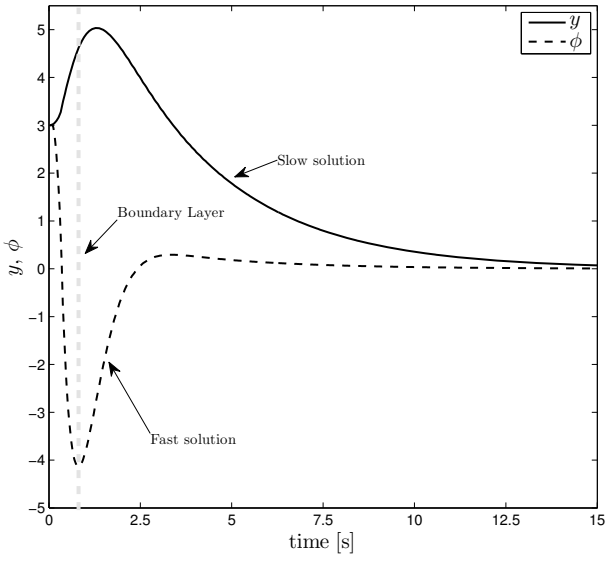

Fig. 1. The state ϕ (the fast dynamics), converges faster than the state y (the slow dynamics). The boundary layer exists near the initial condition.

The fast and slow control, (25) and (18) respectively, are shown in Fig. 3. Where the fast control presents a faster response regarding the slow control. Such controller corresponds to $\epsilon = 0.5$.

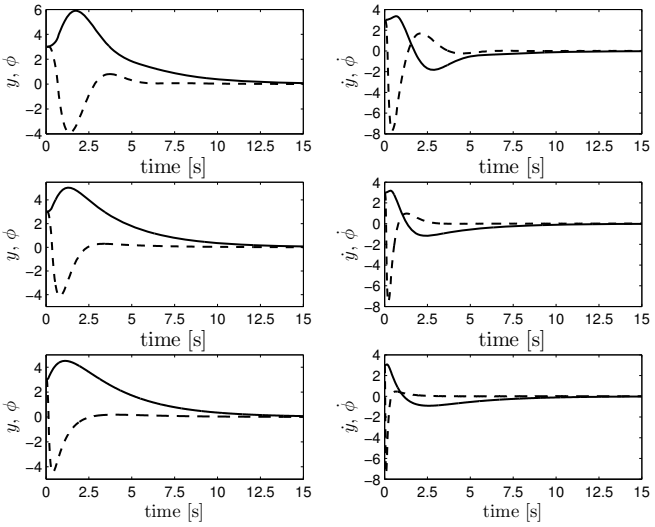

Fig. 2. The states corresponding to the fast dynamics ($(\dot{\phi}, \phi)$: dashed line) converge faster than the states corresponding to the slow dynamics ($(\dot{y}, y)$: solid line). Depending on the value of ϵ, the convergence is faster. In addition, the size of the boundary layer, shown in Fig. 1, is proportional to ϵ.

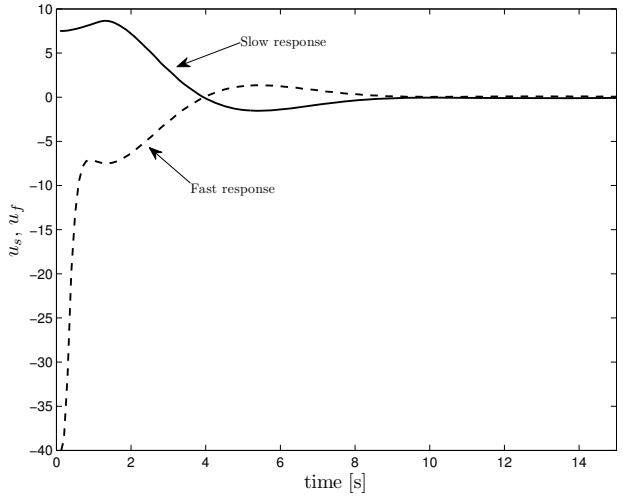

Fig. 3. Slow control u_s is represented by the solid line while the fast control u_f is represented by the dashed line. The time scale separation property is also presented on both controllers.

B. Experimental Results

The proposed controller has been tested on the *Quad-Plane* experimental platform illustrated in Fig. 4. With the Quad-plane at $y = 0$, $\dot{y} = 0$, the desired position is set to $y = 0$, during 40 seconds.

The experiment consist in an autonomous landing, after the vehicle needs to go forward on x, following a line on the floor using its embedded visual system, while maintaining a y relative position equal to zero w.r.t. the estimated line. Thus, the desired position and orientation in the roll dynamics and y-position is zero.

Fig. 5 illustrates the behavior of the proposed controller, in which the vehicle is stabilized on the desired position. The Quad plane is disturbed on the roll angle at $t = 32$ sec. as it is shown in Fig. 5. The system has been disturbed in order

to show the rapid response on the fast dynamics represented by the pitch dynamics $(\phi, \dot{\phi})$ in comparison with the slow dynamics represented by the the position dynamics $(y, \dot{y})$.

Fig. 4. Quad-plane experimental platform, developed at HEUDIASYC laboratory.

As we see in Fig. 5, the performance of the controller is satisfactory.

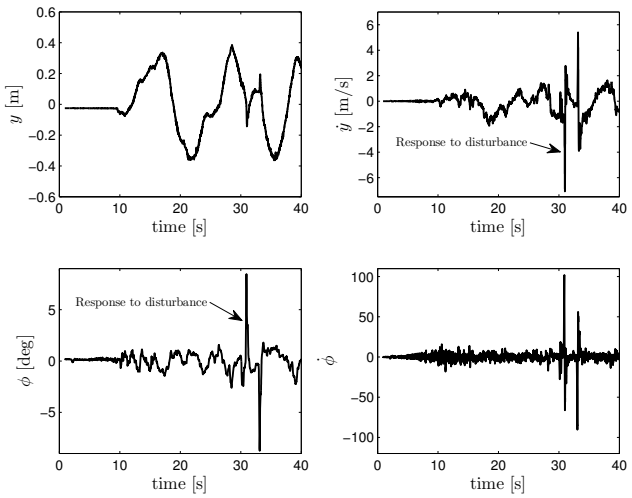

Fig. 5. Experimental results showing the effectiveness of the controller. In the first row the translational dynamics is shown while in the second row the rotational dynamics is illustrated. Beyond the inherent noise, the response in translational dynamics behaves slower than the rotational dynamics. We have disturbed the vehicle on the roll angle at $t = 32$.

VI. Conclusion

A controller based on the singular perturbation approach has been proposed so that the closed loop behavior achieves the desired performance. We have associated the translational displacement with the slow dynamics and the rotational displacement with the fast dynamics. For this purpose we have introduced the parameter ϵ on the dynamic equations. The introduction of this parameter leads to a time-scale separation of the MAV system. A Lyapunov function was proposed for the entire system and stability of the closed loop system was proved for all $\epsilon < 1$.

The Lyapunov-based controller using singular perturbation theory has been tested in numerical simulations. The controller has been also successfully applied to a Quad-plane experimental platform showing good performance.

References

[1] S. Bouabdallah and R. Siegwart, "Backstepping and sliding-mode techniques applied to an indoor micro quadrotor," in *In Proceedings of IEEE Int. Conf. on Robotics and Automation*, Barcelona, Spain, Apr. 2005, pp. 2247–2252.

[2] D. Cabecinhas, R. Cunha, and C. Silvestre, "Saturated output feedback control of a quadrotor aircraft," in *Proc. IEEE American Control Conference (ACC'2012)*, Montréal, Canada, Jun. 2012, pp. 4667–4672.

[3] T. Lee, M. Leok, and N. H. McClamroch, "Nonlinear robust tracking control of a quadrotor uav on se(3)," in *Proc. IEEE American Control Conference (ACC'2012)*, Montréal, Canada, Jun. 2012, pp. 4649–4654.

[4] G. Flores, L. Garcia, G. Sanahuja, and R. Lozano, "Pid switching control for a highway estimation and tracking applied on a convertible mini-uav," in *Proc. 51st IEEE Conference on Decision and Control (CDC'2012)*, Maui, HI, USA, Dec. 2012, to be published.

[5] E. Altuğ, J. P. Ostrowski, and C. J. Taylor, "Control of a quadrotor helicopter using dual cameravisual feedback," *The International Journal of Robotics Research*, vol. 24, no. 5, pp. 329–341, 2005.

[6] G. Flores, J. Escareno, R. Lozano, and S. Salazar, "Quad-tilting rotor convertible mav: Modeling and real-time hover flight control," *Journal of Intelligent and Robotic Systems*, vol. 65, no. 1-4, pp. 457–471, 2012.

[7] L. G. Carrillo, G. Flores, G. Sanahuja, and R. Lozano, "Quad-rotor switching control: An application for the task of path following," in *Proc. IEEE American Control Conference (ACC'2012)*, Montréal, Canada, Jun. 2012, pp. 4637–4642.

[8] D. S. Naidu and A. J. Calise, "Singular perturbations and time scales in guidance and control of aerospace systems: A survey," *Journal of Guidance, Control and Dynamics*, vol. 24, no. 6, pp. 1057–1078, 2001.

[9] S. Esteban, J. Aracil, and F. Gordillo, "Lyapunov based asymptotic stability analysis of a three-time scale radio/control helicopter model," in *AIAA Atmospheric Flight Mechanics Conference and Exhibit*, Honolulu, Hawaii, Aug. 2008.

[10] S. Bertrand, T. Hamel, and H. Piet-Lahanier, "Stability analysis of an uav controller using singular perturbation theory," in *Proceedings of the 17th World Congress The International Federation of Automatic Control*, Seoul, Korea, Jul. 2008, pp. 5706–5711.

[11] B. Etkin and L. Reid, *Dynamics of Flight Stability and Control*. John Wiley and Sons, 1996.

[12] M. Oishi and C. Tomlin, "Switching in nonminimum phase systems: Application to vstol aircraft," in *Proc. IEEE American Control Conference (ACC'2000)*, Chicago, IL, Jun. 2000, pp. 838–843.

[13] R. Mahony and T. Hamel, "Robust trajectory tracking for a scale model autonomous helicopter," *International Journal of Robust and Nonlinear Control*, vol. 14, no. 12, p. 1035Ű1059, 2004.

[14] P. Kokotović, H. K. Khalil, and J. O'Reilly, *Singular Perturbation Methods in Control: Analysis and Design*. London: Academic Press: Siam, 1999.